



Design of self-healing styrene-butadiene rubber compounds with ground tire rubber-based reinforcing additives by means of DoE methodology

Karina C. Nuñez Carrero^{a,b,*}, Luis E. Alonso Pastor^a, Marianella Hernández Santana^{c,*}, José María Pastor^{a,b}

^a Department of Condensed Matter Physics, University of Valladolid, Paseo de Belén, 7, 47011 Valladolid, Spain

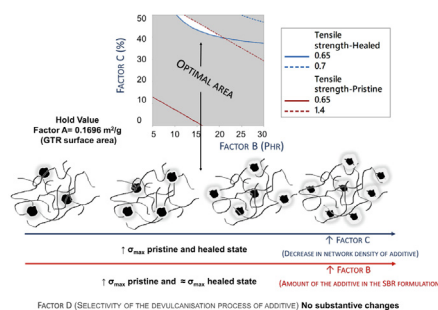
^b Foundation for Research and Development in Transport and Energy (CIDAUT), Parque Tecnológico de Boecillo, Plaza Vicente Aleixandre Campos 2, 47051 Valladolid, Spain

^c Institute of Polymer Science and Technology (ICTP), CSIC, Juan de la Cierva 3, 28006 Madrid, Spain

HIGHLIGHTS

- Two full factorial designs to establish the relationship between microstructure and mechanical performance.
- The tensile strength can be modelled by the factorial full design with high predictive capability.
- The decrease in network density of devulcanised tire residue were statistically more important factor.
- Selective network breakage of devulcanised tire residue was negligible.

GRAPHICAL ABSTRACT



ARTICLE INFO

Article history:

Received 23 May 2022

Revised 28 June 2022

Accepted 28 June 2022

Available online 30 June 2022

Keywords:

Mechanical properties

Self-healing

Styrene-butadiene rubber (SBR)

Factorial design

Ground tire rubber

ABSTRACT

In the effort to find a balance between the mechanical properties of self-healing styrene-butadiene rubber (SBR) compounds, before and after a macroscopic damage, a study based on the use of devulcanised tire residue (dGTR) as reinforcement has been carried out. Two full factorial designs and their analysis of variance (ANOVA) were used to overcome the challenge of relating the multiple microstructural variables of dGTR to the mechanical properties of the compounds in pristine and healed states. The design of experiments (DoE) predict that the use of dGTR-based reinforcements, with a decrease in network density higher than 50%, enables the incorporation of more than 40 phr of reinforcing filler, increasing the tensile strength in the pristine state (more than 4 times) and mitigating its negative effect on the healing process. Experimental tests have validated these theoretical predictions. This research demonstrates that it is not necessary to control the selectivity of the devulcanisation process. Therefore, it has been demonstrated that only by increasing the dGTR surface network density breakage it is possible to incorporate significant amounts of the residue from simple recycling processes in order to improve the performance of high value-added rubber formulations, such as self-healing materials.

© 2022 The Authors. Published by Elsevier Ltd. This is an open access article under the CC BY-NC-ND license (<http://creativecommons.org/licenses/by-nc-nd/4.0/>).

* Corresponding authors at: Department of Condensed Matter Physics, University of Valladolid, Paseo de Belén, 7, 47011 Valladolid, Spain (Karina C. Nuñez Carrero).

E-mail addresses: karinacarla.nunez@uva.es (K.C. Nuñez Carrero), marher-na@ictp.csic.es (M. Hernández Santana).

1. Introduction

The concept of self-healing in polymers first appeared with the studies of White et al. [1] in 2001. Their work reported a structural polymeric material with the ability to autonomously repair cracks. The material incorporated a microencapsulated healing agent that

was released upon crack intrusion. The polymerisation of the healing agent was then triggered by contact with an embedded catalyst, which bonded the crack faces together. Since then, research focused on self-healing materials [2,3] and, especially, self-healing rubbers with the pioneering work of Cordier et al. [4], has rapidly expanded with new concepts and strategies being developed in academic and industrial laboratories around the world.

One of the main concerns that have emerged during all these years of research is related to improving the mechanical, thermal, and electrical behaviour of these self-healing materials, both in their pristine and healed state, as well as achieving high restoration efficiencies. In this sense, many authors have used fillers of different natures. One example is graphene [5–7]. Some authors reported excellent restoration of thermal and electrical conductivity with nanofiller content; however, graphene-polymer interactions at the healed interface limit the achievement of high tensile strength restoration. Other authors have used nanoclays such as attapulgite (AT) in self-healing polyurethanes [8]. Their results indicated the importance of controlling the amount of AT in order to maintain a positive balance between healing and mechanical properties. Kuang et al. [9] have also reported the use of carbon nanotubes (MWCNTs) in self-healing rubber matrices. To improve the antagonistic effect of the filler on the mechanical properties and healing efficiency, these researchers modified MWCNTs with furfuryl-terminated groups (MWCNT-FA). By this means, the filler was able to play a dual role; as an effective reinforcing agent on one hand, and as a healing precursor on the other hand. This was due to the better dispersion and compatibilisation of the filler into the matrix.

The use of ground tire rubber (GTR) can also be considered as alternative filler to reinforce self-healing rubbers. It is a strategy that responds to two challenges: i) the technical one that looks for a balance between mechanical performance and healing efficiency; and ii) the environmental one, giving a second life to secondary materials in high value-added applications. Hernandez et al. [10] were pioneers on the development of self-healing styrene-butadiene rubber (SBR) compounds with GTR. They reported good mechanical performance without affecting the healing efficiency by using silane-based coupling agents. In a recent publication [11], it was informed of devulcanised GTR (dGTR) as a possible reinforcing agent in self-healing SBR formulations. In this study, it was demonstrated that regardless of the applied devulcanisation process (thermodynamical, chemical, microwave), the presence of free chains on the surface of dGTR can be an effective substitution of any compatibiliser or surface treatment of the GTR for enhancing the filler-matrix adhesion. However, even though there is a great deal of current interest in devulcanisation processes [12,13] it is not clear which microstructural characteristics of dGTR are the most effective and how this condition can be optimised, depending on the application.

It is challenging to separate the microstructural characteristics of dGTR, such as decreasing network density and selectivity of surface chain breakage. It is necessary to study them individually in order to establish which parameter has a greater influence on the mechanical properties of the self-healing compounds, both in their pristine and healed state. Thus, this research proposes a study based on the Design of Experiments (DoE) methodology to establish the correct relationship between them, understanding the complexity of both the dGTR microstructural variables and the analysed responses (mechanical properties and healing efficiencies).

The DoE approach is traditionally used in materials engineering as it provides a way to reveal which factors influence the response of an experiment. This approach attempts to present predictive knowledge about complex, multivariable problems with few

attempts [14]. DoE is a statistical technique that enables us to determine and understand how certain factors influence the variables of interest, reaching valid and objective conclusions. It consists of running a series of tests in which deliberate changes are induced in the input variables to a process, in such a way that it is possible to identify the causes of the changes in the chosen output response [15]. DoE is highly effective in processes where their performance is affected by a number of factors.

Other authors have proposed factorial experimental designs to study tire residue in different fields: for example, to optimise its devulcanisation process, using supercritical CO₂ [16,17], to study polyolefin/GTR formulations [18] for foaming processes or predicting mechanical behaviour of elastomeric formulations [19]. In all these cases, the experimental process parameters were studied as inputs, without the microstructural factors of the GTR being part of the analysis. In this research, a full factorial design is proposed for the first time to generate sufficient knowledge on the relationship between dGTR microstructure (input) and the mechanical properties of self-healing SBR compounds (in both pristine and healed state). The main goal is to find the ideal microstructure as to improve the mechanical response of self-healing SBR compounds. The results obtained will enable dGTR to be modified accurately in order to be considered as a high value-added recycled additive.

2. Experimental

2.1. DoE methodology

Experiments were conducted based on the full factorial design approach. It consists of all possible combinations of several levels of factors, obtaining information about the main effects [15,20]. Experiments were designed using a 2⁴ full factorial design, i.e., 4 factors with 2 levels each. The statistical software Minitab® was used to generate DoEs, and ANOVA was employed for examining the experimental data.

The intrinsic microstructural characteristics of the GTR (surface area of the particles, decrease in network density, and selectivity of the rubber network breakage), as well as the amount used in the formulations, were considered as independent variables at two levels; and the mechanical properties as the dependent variable or response parameter. As the formulations had self-healing properties, the responses were evaluated in both the pristine and healed states.

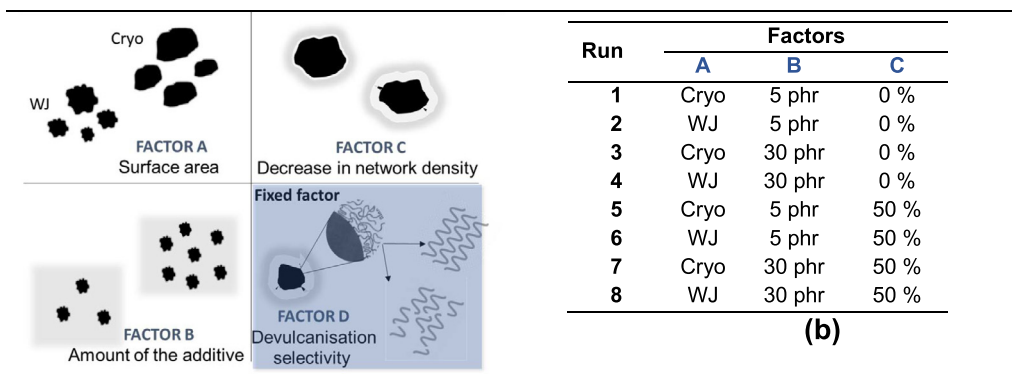
The factors and their selected levels for the preliminary DoE are presented in Fig. 1(a): surface area, amount in parts per hundred rubbers (phr), decrease in network density (%) and selectivity quantifying full devulcanisation (%). The resulting combination of experiments is presented in Supporting Information S1. Due to the microstructural complexity of the studied additive, it was not possible to carry out all the experiments proposed by the 2⁴ factorial designs. Two factors intrinsic to the microstructure of the GTR were studied in separate DoEs (the decrease in network density in DoE 1 and the selectivity of the elastomeric network breakage in DoE 2, resulting in a 2³ and 2² full factorial, respectively (see Fig. 1(b) and 1(c)).

Data for the outcome of each mechanical property were generated in triplicate at each level; therefore, the full factorial design consisted of 24 and 16 runs for DoE 1 and DoE 2, respectively. All the experiments were carried out randomly, avoiding bias in measurements.

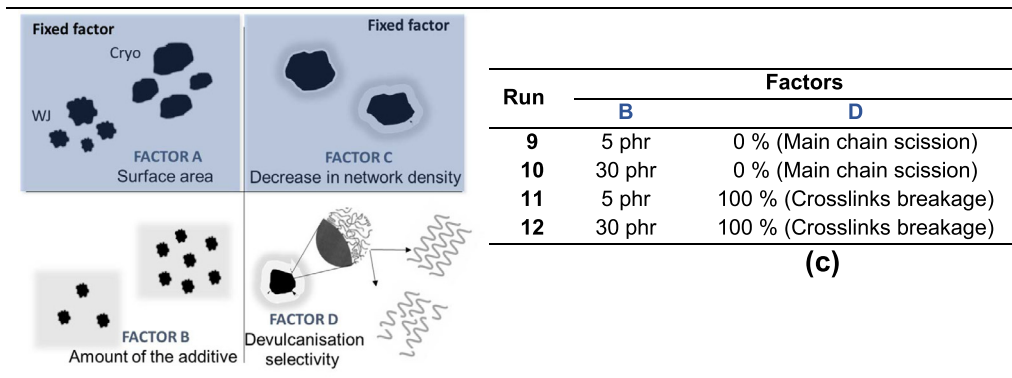
Statistical analysis included ANOVA for determining the significance of each independent variable, its interactions, main effect and interaction plots. The general regression linear model used for the experimental design was:

	Factors	Levels	Domains
A	Surface area of additive	-1	Cryo. BET:0.0209 m ² /g
		+1	WJ. BET:0.1696 m ² /g
B	Amount of the additive in the SBR formulation	-1	5 phr
		+1	30 phr
C	Decrease in network density of additive	-1	0 %
		+1	50 %
D	Selectivity of the devulcanisation process of additive	-1	0 % (Main chain scission)
		+1	100 % (Crosslinks breakage)

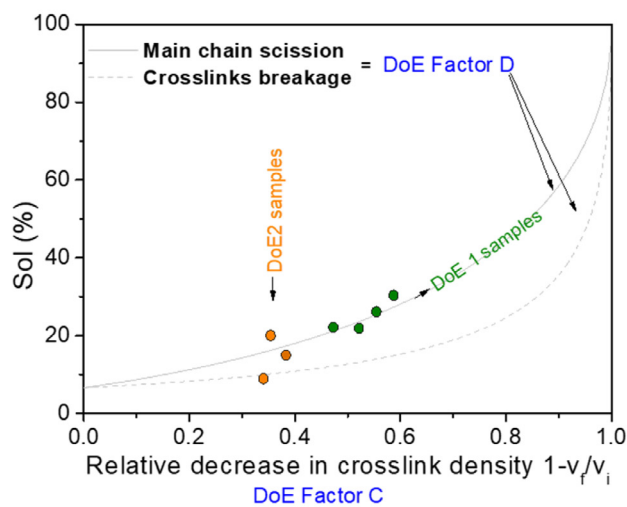
(a)



(b)



(c)



(d)

Fig. 1. (a) DoE's initial approach, (b) DoE 1, (c) DoE 2 and (d) Graphical representation of the additive samples used in DoE 1 and DoE 2 using Horikx's plots.

Table 1
SBR compounds with different crosslink densities used as additives to validate the DoE.

Validation test		Samples of virgin additive		
		S _{0.7}	S ₁	S ₂
Ingredients (phr)	SBR	100	100	100
	ZnO	5	5	5
	SA	1	1	1
	CBS	0.7	1	2
	S	0.7	1	2
Network properties	Crosslink density ($\times 10^{-5}$ mol/g)	0.85	2.76	6.51
	Decrease in network density	87%	57%	0%
	Factor C			

$$y = \beta_0 + \beta_1 x_1 + \beta_2 x_2 + \dots + \beta_{12} x_1 x_2 + \dots + \varepsilon \quad (1)$$

where y is the response; x_1 and x_2 are the variables; β_0 is the constant term; β_1 and β_2 are the coefficients of the polynomial for linear effects; β_{12} is the coefficient of the polynomial for the interaction effect and ε represents the error term.

2.2. Materials and methods

2.2.1. Ground tire rubber (GTR)

Rubber granules from end-of-life truck tires were used. Two grinding technologies were further employed, cryogenic and water jetting grinding. Cryogenic GTR (Cryo) was supplied by Lehigh Technologies and GTR from water jet technology (WJ) by Rubber Jet. Both GTR were selected having the same particle size range. Details on the particle size and composition of the as-received granules and the resulting ground material (powder) are reported in [Supporting Information S2](#).

2.2.2. dGTR-based additives

Thermo-mechanical devulcanisation was selected for obtaining the additives required in the DoEs. The devulcanisation was carried out in an internal mixer (Haake, model Rheomix 3000p) with a fill volume of 70%, using Banbury type rotors at room temperature and at a rotor speed of 30 rpm for 10 min. To obtain different microstructures, setpoint devulcanisation temperatures were varied from 60 °C to 240 °C, with 30 °C intervals. The average temperatures of the samples, recorded by the equipment, were reported. The devulcanisation process slightly modifies the particle size, which implies a change in surface area (Factor A). However, these variations were not considered in the design and only surface differences associated with the grinding process, Cryo or WJ, were considered (see [Supporting Information S2](#)).

The additives obtained from the GTR devulcanisation processes and their characterisation are presented in the [Supporting Information S3](#).

2.2.3. Self-healing SBR compounds

SBR (E-SBR Europrene 1502), and commercial grade vulcanizing additives supplied by Sigma Aldrich, were used as-received. The baseline formulation used was SBR (100 phr), zinc oxide ZnO (5 phr), stearic acid SA (1 phr), N-cyclohexylbenzothiazole-2-sulphide CBS (1 phr), sulphur S (1 phr) and the additive based on GTR was added according to the specifications of the DoEs. Mixing was performed in an open two-roll mill (Comerio Ercole, model MGN-300S) at room temperature using a rotor speed ratio of 1:1.5. First, rubber was passed through the rolls until a band was formed. The activating complex (ZnO and SA) and GTR-based additive were then progressively added to the rubber and, finally, ending with the curatives (CBS and S).

The crosslinking process was followed using a Rubber Process Analyzer (Alpha Technologies, model RPA2000) at curing temperature $T_c = 160$ °C, frequency 0.833 Hz and 2.79 % strain for 60 min.

The composites were then vulcanized in an electrically heated hydraulic press (Gumix) at 160 °C and 200 MPa according to their t_{90} as derived from the corresponding curing curves. Samples were cut out from press-cured sheets to perform all the characterization and testing.

2.2.4. Validation and optimisation of DoEs

To validate the ANOVA interpretation and to assess the influence of parameters such as heterogeneity and contamination of the GTRs (recycled material), three additives from virgin rubber with different crosslink densities were prepared. For this purpose, the sulphur content was varied, keeping the system semi-efficient (accelerant/sulphur ratio = 1). [Table 1](#) shows the formulations prepared and the characteristics of the network obtained. The resulting material was subjected to a WJ grinding process (BET: 0.1870 m²/g). Self-healing SBR compounds with 20 phr of these additives (S_{0.7}, S₁ and S₂) were obtained and characterised.

The conditions used for the optimisation experiments are listed in [Table 2](#). These experiments were set up by selecting combinations of independent variables outside the experimental domain. The predictive power of the models was tested in the optimal zone: Factor A: WJ, Factor B > 30%, Factor C > 50%. Thus, the experiments were conducted without taking Factor D into account.

2.3. Characterization

2.3.1. Additive characterization

Sol fraction (Sol %): About 5 g of GTR or dGTR were weighed (W_{sample}) and subjected to Soxhlet extraction in acetone for 24 h and then in toluene for 72 h. The sol fraction was defined as the sum of the soluble fractions in acetone and toluene (see [Supporting Information S3](#)).

Crosslink density: The crosslink density was determined through equilibrium swelling experiments [21]. About 0.2 g of the acetone extracted sample were placed in toluene at room temperature and in darkness -to avoid molecular changes- for 72 h. The toluene was refreshed every 24 h in order to ensure equilibrium swelling. The swollen samples were taken out from the solvent, carefully removing any solvent excess and then weighed again. After that, samples were dried at 45 °C until constant weight (48 h). Crosslink density

Table 2
SBR compounds used for optimisation tests.

Ingredient (phr)	Optimisation tests			
SBR	100	100	100	100
ZnO	5	5	5	5
SA	1	1	1	1
CBS	1	1	1	1
S	1	1	1	1
dWJ_200°C Factor B	10	20	30	40
dWJ_200°C Factor C	63%	63%	63%	63%

was calculated using the Flory–Rehner equation [22] considering tetra-functional crosslinks (see [Supporting Information S3](#)).

Horikx plots: Horikx derived a theoretical relationship between the soluble fraction generated after degradation of a polymer network and the relative decrease in crosslink density, as a result of either main-chain scission or crosslink breakage [23]. A quantitative value of the network rupture and the selectivity of the devulcanisation process can be estimated from the Horikx diagrams, calculating a percentage of devulcanisation according to the methodology proposed by Edwards et al. [24,25] (see [Supporting Information S3](#)).

Optical microscopy: The distribution and dispersion of the fillers in the SBR compounds were analysed with an optical microscope (Olympus, model BX60 M).

BET surface area: BET surface area of GTR powder was determined by nitrogen volume adsorption at $-196\text{ }^{\circ}\text{C}$ using a surface area and porosity analyser (Micromeritics, model ASAP2020). GTR was vacuum previously dried at $80\text{ }^{\circ}\text{C}$.

3.2. Self-healing rubber compounds characterization

Tensile testing: Dog-bone shape specimens were used for uniaxial tensile testing. Tests were done on a universal mechanical testing machine (Instron, model 2530-416) equipped with a 1 KN load cell. Samples were stretched until failure at a constant crosshead speed of 200 mm/min at room temperature. Stress at break (ultimate stress) and strain at break (ultimate strain) were determined in order to mechanically characterize the SBR compounds.

Healing protocol: Dog-bone specimens were manually cut in the center with the aid of a razor blade, creating a proper joining area. In order to heal the specimens, the two separated parts were carefully repositioned together and fastened with clamps. Then, they were placed in an oven at $130\text{ }^{\circ}\text{C}$ for 1 h. The thermally treated specimens were subjected to a tensile test applying the previous testing conditions. Healing efficiency (η) was calculated by Eq. (2):

$$\eta(\%) = \frac{P_{\text{Healed}}}{P_{\text{Pristine}}} \cdot 100 \quad (2)$$

where P is the mechanical property (Young's modulus, elongation at break or maximum tensile stress) of the healed and pristine specimens determined under the same test conditions.

3. Results and discussion

3.1. DoEs methodology and ANOVA interpretation

3.1.1. Factorial design

The applied factorial design considers that the microstructural characteristics of GTR are complex (the composition depends on the source and the recycling processes to which it was exposed, the particle size, the surface area, the state of the cross-linked network, etc.). This study has focused on three determining factors: the surface area of the particles (Factor A), the decrease in network density (Factor C) and the selectivity of the elastomeric network breakage (Factor D), trying to keep the rest of the microstructural and compositional characteristics of the GTR fixed. In addition, a macrostructural factor of the final formulation was considered: the amount of additive used (Factor B).

Some approximations were made to overcome the limitations encountered when feeding the DoEs. Firstly, it was not possible to obtain all the combinations that would result from the study of the four factors (see [Fig. 1a](#)). Some of the combinations were inconsistent due to the specific nature of the reinforcement studied (i.e., 0% decrease in network density and 100% crosslink breakage, see [supplementary information S1](#)). In order to adequately address the experimental aspect, it was decided to use the strategy of

designing two independent DoEs (see [Fig. 1\(b\)](#) and [1\(c\)](#)), which could also provide a separate view of microstructural Factors C and D (associated with particle devulcanisation). Secondly, after obtaining the different dGTR samples, the two factors (C and D, decrease in network density and selectivity of the devulcanisation process, respectively) were determined by the Horikx's plots (see [Supporting Information S3](#)). However, this relationship is designed for unfilled elastomeric samples. This means that the values presented are indicative, as GTRs have significant amount of fillers (mainly carbon black). It was also difficult to select dGTR particles with the exact combination of C and D required by the proposed design. Some approximations were assumed and are presented in [Table 3](#).

It is important to point out that the chosen control mechanical properties (responses variables) are consistent with those studied in the literature for self-healing elastomers, with two levels of response: one for the pristine state and the other for the healed state. Therefore, the aim is not only to associate the DoEs factors with the maximization of the mechanical properties at both states, but also to reach maximum healing efficiencies, which, as reported in the literature, are usually antagonistic [26]. The complexity of the factors and the responses of these DoEs describe an intricate challenge that is summarized in this methodology. The results obtained should be interpreted as a qualitative guide for the design of self-healing compounds. The total number of experimental runs for the full factorial design, the mechanical properties of both pristine and healed state, standard deviation (St Dev) and healing efficiency of all the test results are shown in [Table 3](#).

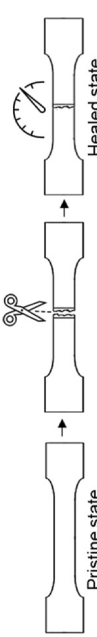
3.1.2. General full factorial results

The Pareto charts of the standardized effects (see [Fig. 2](#)) have a red line to point out which effects are statistically significant, i.e., bars crossing the reference line are statistically significant. The reference line for statistical importance depends on the level of significance, indicated by the " α " value [27]. A 95% confidence level ($\alpha = 0.05$) was used in this study. Additionally, the results of the Pareto charts show the absolute values of the standardised effects from the highest to the lowest effect.

As can be seen in [Fig. 2](#), for properties such as Modulus at 50% strain and elongation at break, none of the control factors studied were significant, neither in the pristine nor in the healed state, neither in DoE 1 nor in DoE 2. In the case of the Modulus, the fed response corresponds to values at very low strains (50%); it was not possible to measure this property at higher strains in all specimens (pristine and healed), due to their premature failure. The values reported are practically invariant at these strain levels, so that statistically no factor studied can introduce significant changes. Another possible explanation, at a statistical level, is associated with the fact that all the factors are possibly significant in equal degree and it is not likely to rank them in order of importance. This possibility may explain the complex behaviour of the elongation at break. Multiple trends have been reported about the effect of GTR on the elongation at break of rubber compounds: it can stop or deflect the crack path, resulting in a stabilised or higher deformation [28]; it can even act as a plasticiser as a result of the additives (i.e., oils) [29] that the GTR may retain. On the contrary, GTR particles can also act as stress concentrators, limiting the deformation capacity of the rubber [30]. Unfortunately, these DoEs are not able to associate these two opposite effects to the microstructure of the dGTR used. However, DoEs have been able to predict the influence of the microstructural factors on the tensile strength (see [Fig. 3](#)). Interestingly, this is the most analysed and reported property in self-healing rubber compounds [10,11,31].

Table 3
Experimental runs and their responses (Mechanical properties).

Statistical experiments:



RUN	DoE	FACTOR			Responses:													
		A	B (phr)	C (%)	D (%)	Pristine					Healed							
						M _{50%} (MPa)	M _{100%} (MPa)	σ _b (%)	σ _{max} (MPa)	M _{50%} (MPa)	M _{100%} (MPa)	σ _b (%)	σ _{max} (MPa)	η (%) ^a	M _{50%}	M _{100%}	σ _b	σ _{max}
DoE 1	1	Cryo	5	0	0	0.45 ± 0.02	0.58 ± 0.02	521.0 ± 10.6	1.15 ± 0.06	0.45 ± 0.02	0.55 ± 0.03	59.5 ± 4.0	0.56 ± 0.04	100	95	11	48	
	2	WJ	5	0	0	0.47 ± 0.01	0.59 ± 0.01	403.3 ± 9.0	1.34 ± 0.01	0.52 ± 0.01	0.59 ± 0.01	82.4 ± 3.8	0.63 ± 0.00	110	100	20	47	
	3	Cryo	30	0	0	0.40 ± 0.01	0.41 ± 0.01	240.8 ± 15.9	0.45 ± 0.03	0.42 ± 0.01	-	76.3 ± 1.3	0.40 ± 0.04	105	-	32	89	
	4	WJ	30	0	0	0.48 ± 0.02	0.58 ± 0.04	457.3 ± 26.8	1.36 ± 0.06	0.50 ± 0.01	-	58.7 ± 3.4	0.51 ± 0.01	104	-	13	37	
	5	Cryo	5	50 (~59)	0 (~15)	0.46 ± 0.01	0.57 ± 0.02	403.5 ± 21.2	1.21 ± 0.04	0.49 ± 0.01	-	91.1 ± 4.5	0.62 ± 0.01	106	-	23	51	
	6	WJ	5	50 (~41)	0 (~0)	0.44 ± 0.02	0.57 ± 0.02	428.5 ± 15.4	1.30 ± 0.05	0.50 ± 0.02	0.64 ± 0.02	98.4 ± 3.6	0.65 ± 0.02	113	112	23	50	
	7	Cryo	30	50 (~59)	0 (~15)	0.46 ± 0.02	0.54 ± 0.02	714.2 ± 46.9	2.12 ± 0.15	0.49 ± 0.01	0.61 ± 0.04	120.3 ± 9.9	0.66 ± 0.02	106	113	17	31	
	8	WJ	30	50 (~41)	0 (~0)	0.42 ± 0.01	0.48 ± 0.01	631.1 ± 47.8	1.38 ± 0.09	0.47 ± 0.01	0.57 ± 0.01	187.6 ± 14.4	0.77 ± 0.04	111	119	30	56	
DoE 2	9	WJ	5	35 (~41)	0 (~0)	0.44 ± 0.02	0.57 ± 0.02	428.5 ± 15.4	1.30 ± 0.03	0.50 ± 0.02	0.64 ± 0.02	98.4 ± 3.6	0.65 ± 0.02	113	112	23	50	
	10	WJ	30	35 (~41)	0 (~0)	0.42 ± 0.01	0.48 ± 0.01	631.1 ± 47.8	1.38 ± 0.09	0.47 ± 0.01	0.57 ± 0.01	187.6 ± 14.4	0.77 ± 0.04	111	119	30	56	
	11	WJ	5	35 (~31)	100 (~100)	0.46 ± 0.01	0.58 ± 0.01	409.9 ± 12.2	1.30 ± 0.05	0.54 ± 0.03	-	75.2 ± 3.9	0.63 ± 0.01	117	-	18	48	
	12	WJ	30	35 (~31)	100 (~100)	0.49 ± 0.01	0.56 ± 0.01	477.4 ± 19.8	1.37 ± 0.05	0.50 ± 0.04	-	65.4 ± 5.3	0.56 ± 0.02	102	-	14	41	

^a Standard deviation (St Dev) < 0.1

3.1.3. Statistical analyses and model adequacy for tensile strength

The ANOVA (see Table 4) summarises the statistical analyses of the DoEs responses corresponding to tensile strength. The associated probability values (p-values) for the factors and levels of each DoE can be observed. Only the p-values that are less than 0.05 are shown; this means that, in the selected cases, it is possible to reject the null hypothesis, i.e., that there is a statistically meaningful difference between the tests conducted, the variables and the combinations between them. The probability is near zero, indicating that the test results are not affected if there is any change in the variables. Factors and interactions without any statistical meaning were grouped as part of the error [15].

It was only possible to obtain the ANOVA of the dependent variable (tensile strength) in the pristine and healed state for DoE 1, and for the pristine state in DoE 2 (See Table 4). It should be noted that in all cases, Factor B and its interactions are significant; in DoE 1 Factor C (decrease in network density) showed the lowest p-values and in DoE 2 no significance could be found for Factor A and D (surface area and devulcanisation selectivity, respectively). After eliminating the non-significant coefficients, the regression model was obtained fitted in terms of the real variables with their levels for each response [32]. The values of the coefficients and their relevance were also included in the outputs of these mathematical models. In all linear models, the maximum coefficient had the highest effect on the response, in this case the maximum coefficient was found in Factor C (decrease in additive network density).

Table 4 also compiles the R² values, showing that all of them are above 99%; hence, one can confirm that the model fitting to the experimental data was satisfactory [33]. The small differences between the R² and the R²(adj.) values imply that the regression model is statistically significant and reliable in predicting the tensile strength within the range of studied factors [34]. Equations 3, 4 and 5 show the final results of the best metamodel obtained from the test specimens (see Table 3). These equations translate the response generation capacity of a mathematical model according to the adopted factorial design.

In addition, the adequacy of the model was inspected by residual analysis by means of normal probability plots of the residuals at 95% confidence level for the tensile strength under the conditions studied, as shown in supporting information S4, for each studied response. The analysis of the residuals will determine the accuracy of the model fit by investigating the hypothesis of normality and equality of variance [15]. All the plots have a similar behaviour and reveal that the residuals are quite close to the straight line. i.e., the data are normally distributed, which is a hypothesis in ANOVA analysis [15]. Therefore, the confidence of the ANOVA results and all the information from the experimental data is hereby confirmed.

3.1.4. Main effect and interaction plot for tensile strength in the pristine and healed state

The main effect and interaction plots represent the results of the regression analysis. They show the magnitude and direction of the effects, the mean value of the properties when all experiments in the design are considered (horizontal dotted line in the Fig. 3 (a)), and the mean values of the corresponding variables [27].

In the case of DoE 1, in the pristine state, the use of GTR particles with higher surface area (Factor A) increased the tensile strength. An eight-fold increase of the surface area of the reinforcement additive (from Cryo to WJ) brings about an increase of ~ 40% of the tensile strength (above the average value of the total studied data: 1.1 MPa). Although the same trend is observed in the healed state, only an increase of ~ 10% is found when Factor A (surface area) increases 8 times. It is sufficiently reported in the literature that fillers with low surface area and high dispersion have greater

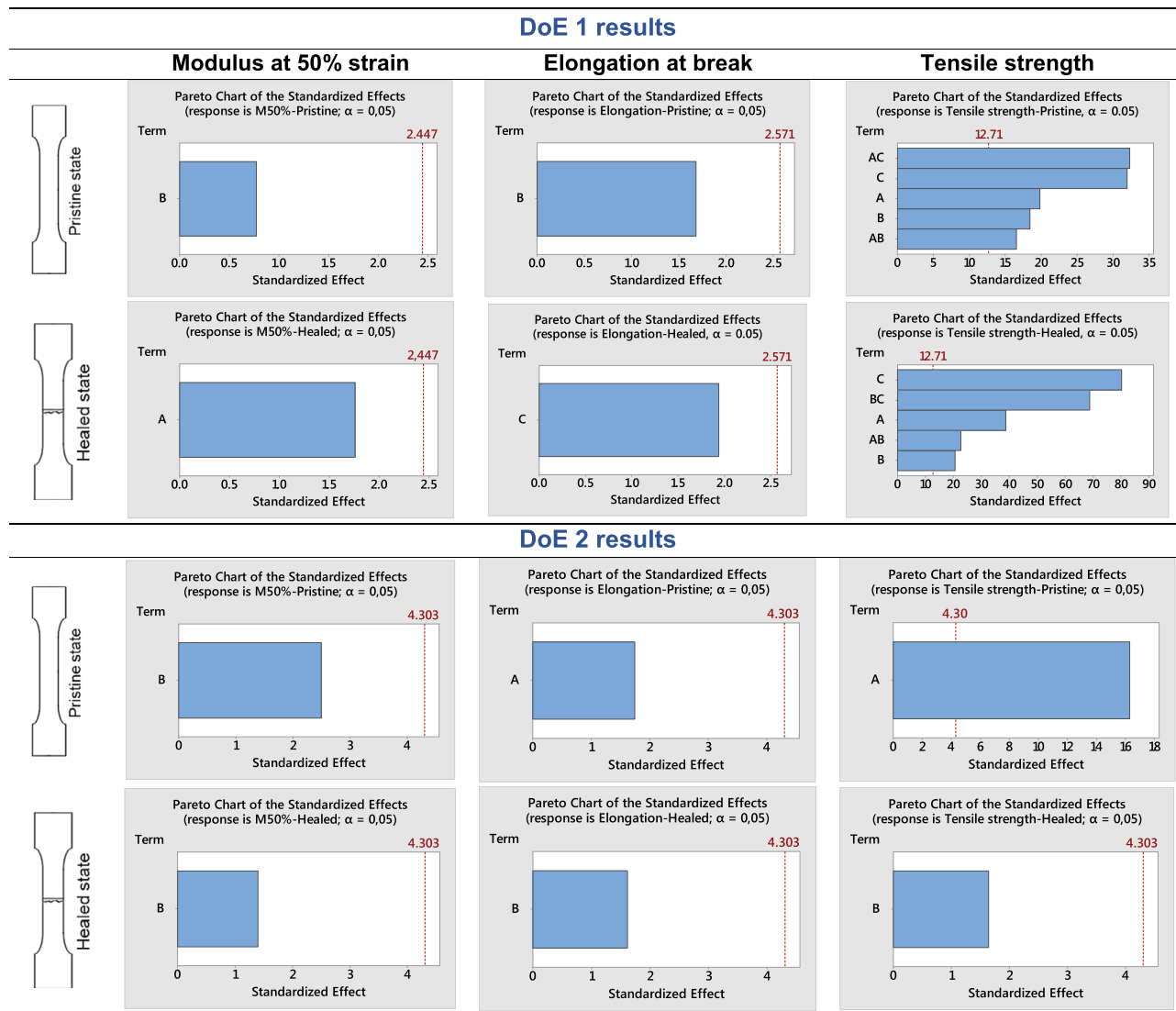


Fig. 2. Pareto charts of standardized effects for measured mechanical properties (responses) in DoE 1 and DoE 2. (Legend: A = Surface area of additive, B = Amount of the additive, C = Decrease in network density and D = Selectivity of the devulcanisation).

interaction with the matrix and therefore, their stiffening effect is enhanced [30,35]. This fact corroborates the importance of Factor A in the use of dGTR. Factor B (amount of additive added in the formulation) shows an antagonistic effect between both states. While in the pristine state, a 6-fold increase in the amount of filler increases the tensile strength by 40%, in the healed state the same increment in Factor B, decreases the tensile strength by 10%. The antagonism is not proportional and the positive effect in the pristine state is more important (see the associated coefficients in equations 3 and 4 in Table 4). In addition to the stiffening effect of GTR in its basal mechanical properties, it has also been demonstrated that the curing behaviour is affected by the presence of GTR, through the migration of sulphur or accelerators between the vulcanised GTR and the matrix [36].

Factor C (associated with the amount of free surface polymeric chains in the particle, resulting from the decrease of the network density) seems to be the most decisive one (higher slope in Fig. 3 (a)), in the pristine and in the healed state. The change from GTR to dGTR with approximately 50% lower network density causes the tensile strength to increase by almost 50% in the pristine state and by approximately 15% in the healed state. Various authors have reported that the use of dGTR instead of GTR in rubber matri-

ces increases the mechanical properties, due to the compatibility generated by the devulcanised surface free chains [28,29].

The overall interpretation of the main effects plots in DoE 1 enables to conclude that the highest tensile strengths are achieved when maximising Factors A, B and C; this means that the best SBR formulation is the one reinforced with 30 phr of WJ type particles and with 50% of its network broken (as confirmed by the values reported for run 8 in Table 3). However, since the standardised Pareto diagrams show interactions with a significant effect between these factors (see Fig. 2), the main effect plots must be completed with the interpretation of the interaction plots.

According to the standardised Pareto diagrams and the ANOVA, the significant interactions for the tensile strength in the pristine state of DoE 1 are AC and AB. Looking at the AC interaction graph (see Fig. 3 (b)), for 0% decrease in network density (blue line), the maximum tensile strength is obtained with high surface area particles (WJ), as predicted by the main effect plots. However, for the 50% decrease in network density (red line) the trend is opposite, with Cryo particles showing the highest tensile strength. This is possibly due to the actual value of the percentage decrease in the network of each of the samples. Although the value set for DoE 1 was 50% (Factor C); the experimental decrease in network density

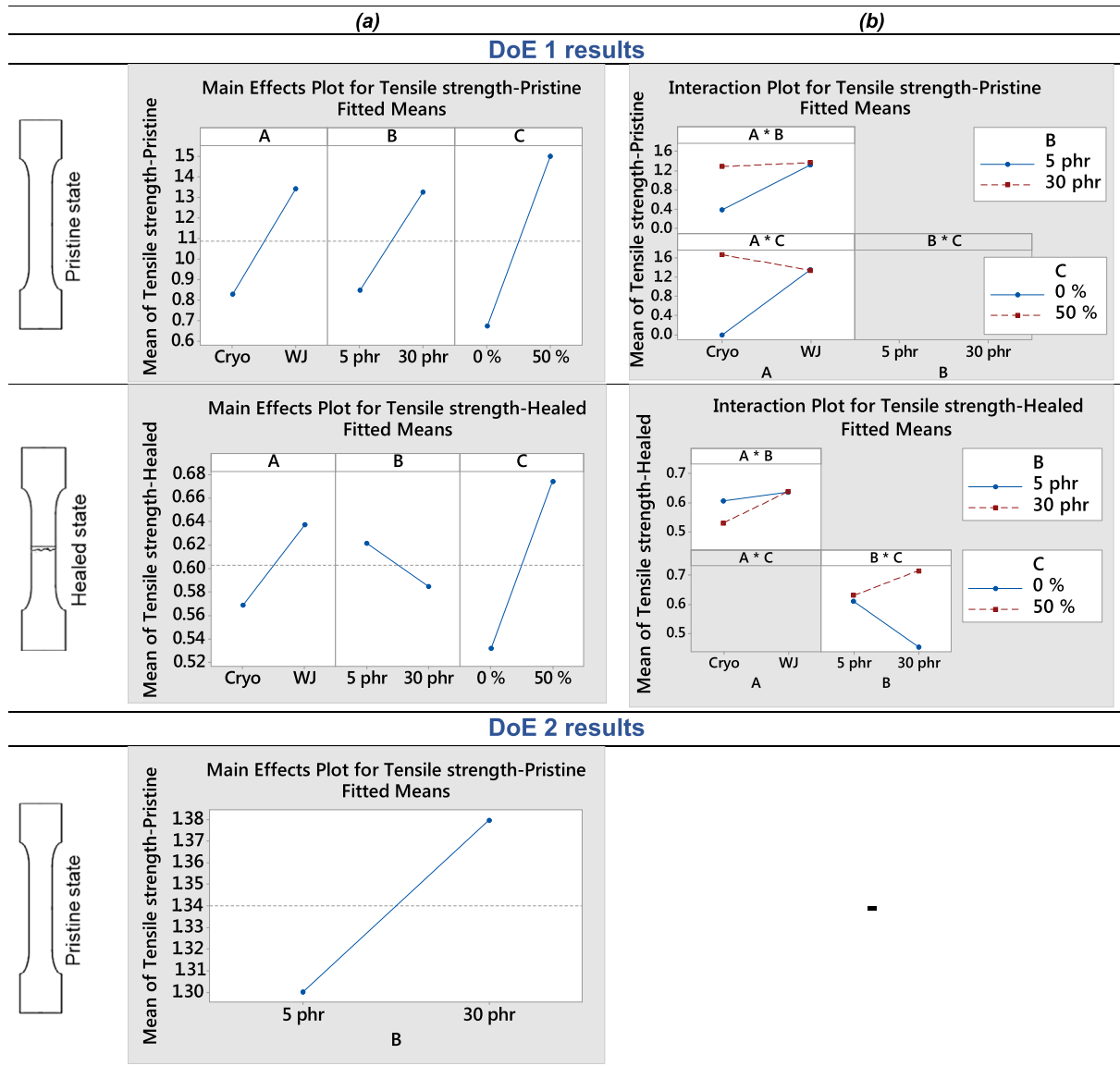


Fig. 3. (a) Main effects plot and (b) Interaction plot for tensile strength.

Table 4

ANOVA for the interaction model of the responses and the general regression linear models with statistical significance for each response.

Term	DoE 1 results		DoE 1 results		DoE 2 results	
	Coef	p-value	Coef	p-value	Coef	p-value
Constant	1.0875	0.008	0.060311	0.001	1.3400	0.000
A	0.2575	0.032	0.003438	0.016	-	-
B	0.2400	0.034	-0.018287	0.031	0.0396	0.004
C	0.4150	0.020	0.071213	0.008	-	-
A*B	-0.2150	0.038	0.020088	0.028	-	-
A*C	-0.4200	0.020	-	-	-	-
B*C	-	-	0.061012	0.009	-	-
R ²	99.94%	-	100%	-	99.25%	-
R ² (adj.)	99.62%	-	99.97%	-	98.88%	-
Linear models						

$$\sigma_{max} = 1.0875 + 0.275A + 0.2400B + 0.4150C - 0.2150A * B - 0.4200A * C(3)\sigma_{max} = 0.0603113 + 0.034388A - 0.018287B + 0.071213C - 0.020088A * B - 0.061012B * C$$

$$(4)\sigma_{max} = 1.3400 + 0.0396B(5)$$

was 59% and 41% for Cryo and WJ samples, respectively (See Table 3). Taking into account the latter and the AC interaction graph, it can be intuited that the decrease in crosslink density has a positive effect on the tensile strength, in the pristine state, which overcomes the effect of the surface area (Factor A). Therefore, the use of dGTR-based reinforcements with high surface area in self-healing SBR formulations only increase the tensile strength if the particles have high network breakage rates. A similar conclusion can be extracted from the AB interaction (see Fig. 3 (b)). The trend of the blue line (5 phr) coincides with the main effects: tensile strength increases as the surface area increases. However, for 30 phr (red line) tensile strength seems to be independent of surface area. This is attributed to the fact that the WJ particles have a lower Factor C value, i.e. a further decrease in the network density at the surface of the particle used. Then, the maximum percentage of dGTR-based filler that can increase the tensile strength in a self-healing SBR formulation, also depends on the decrease in network density.

Regarding the interactions occurring in the healed state in DoE 1, the plots predict the importance of working at low filler concentrations with high surface area particles; but as in the pristine state, the AB interaction (see Fig. 3 (b)) shows that this tendency is conditioned by Factor C. In other words, the tensile strength cannot increase in the healed state using low filler concentration and high surface area, if the dGTR particles do not undergo a high crosslink density decrease. Thus, it was demonstrated that Factor C is also crucial in the healed state. This can be explained by the BC interaction shown in Fig. 3 (b). The red line corresponding to the 50% decrease in network density shows the maximum tensile strength, even at high loading (30 phr), although the latter may be a barrier to the mobility of the rubber chains during repair. This improvement can be attributed to the higher content of disulphide radicals. During the thermo-mechanical devulcanisation, the S-S crosslinks brake, resulting in the formation of disulphide radicals [37]. These radicals are able to rearrange and lead to new interactions, promoting the formation of chemical bonds across the damaged surface [38].

Summarizing, it can be established as a result of DoE 1, that there are two common factors that maximise the tensile strength for the pristine and healed state: Factor A and Factor C (surface area of reinforcement used and the state of the surface network density of them, respectively) the latter being of greater importance. Moreover, the increase of Factor B (amount of particles) and its interactions have an antagonistic effect depending on the state of the compound; in the pristine state it has a proportional effect, while in the healed state it shows and inversely proportional trend. Therefore, Factor B is also decisive for achieving well-balanced properties (i.e., high repair efficiencies), as long as special attention is paid to the network density of the dGTR particles.

Regarding the DoE 2, if Factor C is the most determinant and has been kept fixed in this factorial design, there will be practically no response, as has happened and proven by the standardised Pareto plots and ANOVA. Thus, it has only been possible to obtain a main effects plot for the pristine state, where the next most important factor (Factor B) will be prioritised. This factor follows the same trend described by DoE 1, confirming the consistency of the results obtained in DoE 2.

Some authors have reported that the long free chains resulting from the devulcanisation of GTRs are beneficial, due to their ability to form bonds and/or entanglements with the matrix at the interface [39,40]. However, our experiments show that Factor D (devulcanisation selectivity, i.e. if all free surface chains are preferentially associated with either devulcanisation (100%) or depolymerisation (0%) process), can be neglected in the design of GTR-reinforced self-repairing SBR formulations, possibly because the other factors are more decisive and/or because these long chains do not have

sufficient mobility and polarity to contribute to the repair. Even the results of DoE 2, designed to study almost exclusively Factor D show that in none of the cases do the standardised Pareto diagrams (see Fig. 2) consider it as a statistically important factor. Moreover, the non-standardised Pareto diagrams (see Supporting Information S5), in which all factors are ordered according to their influence, without setting high confidence levels, do not include Factor D or its interactions. It follows that it is a secondary independent variable.

3.1.5. Contour plots

Contour plots are used to graphically explore the three-dimensional relationship between variables in two dimensions [41]. Fig. 4 shows Factor C and Factor B for the DoE 1 plotted on the x and y axis, respectively, and the resistance values represented by contours while keeping constant the value of Factor A (WJ particle). The analysis from the previous section revealed that the decrease in network density is the most significant factor affecting the tensile strength of the formulations in both pristine and healed state. This is consistent with the contour plots: regardless of the amount of additive used, the value is maximised if the decrease in network density is increased. The contours clearly show the possibility of achieving a tensile strength above 2 MPa and 0.7 MPa, in the pristine state and healed state, respectively, if Factor B and C are maximised at the same time. An optimisation methodology

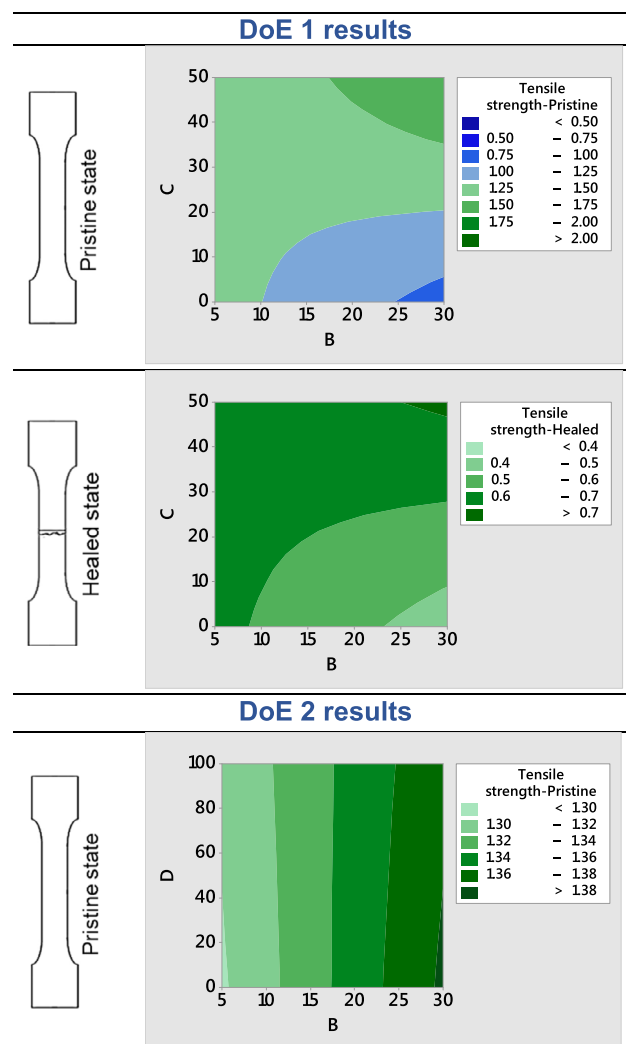


Fig. 4. Contour plots of response vs studied factors for DoEs results.

will be discussed in the next section. The contour plot related to the DoE 2 confirms the independence of the tensile strength values in the pristine state with the selectivity of the network breakage (Factor D), under the conditions studied.

3.2. Validation and optimisation

The interpretation of the results of the factorial designs enabled to establish that the decrease of the network density of the devulcanised GTR particles, used as additive, is a decisive factor in the optimisation of the tensile strength, in the pristine and healed state of SBR compounds. To prove this statement, two experiments were carried out. First, an equivalent additive made from virgin material with different network densities was formulated. The objective was to carry out an experimentation that prioritises Factor C and allows it to be studied in isolation against other factors inherent to a recycled material (i.e., influence of heterogeneity, possible contaminants, reproducibility, etc.). Secondly, an optimisation work was carried out to obtain an additive with a Factor C > 50 % (dWJ_200°C). Using this additive, formulations with >30 phr of reinforcement were evaluated to demonstrate that Factor C > 50 % and Factor B > 30 phr, with particles with high surface area (WJ) can maximise the property studied, as predicted by the ANOVA. Table 5 shows the description of the formulations carried out, the variables studied and the mechanical responses obtained.

3.3. Validation results (Significance of Factor C)

Fig. 5 (a) shows the tensile strength for the pristine (solid line) and healed state (dashed line) of SBR compounds reinforced with two types of additives: virgin (blue line) and recycled (black line). Inherent characteristics of the additive (Factors A, C and D) and the amounts used in the formulations (Factor B) are shown in Table 5. As it can be seen, the trend described by the ANOVA interpretation is validated: the greater the decrease in network density, the greater the increase in tensile strength, independently of the origin of the additive (recycled or virgin). Moreover, this effect is undoubtedly much larger in the pristine state, as predicted by the factorial design.

Meanwhile, there are significant differences on tensile strength when comparing the two types of additives with the same Factor C (i.e., 0%) (blue and black line in Fig. 5 (a)). This is due to the different natures and compositions of the additives used. The recycled additive is composed of a mixture of natural and synthetic rubbers, with high percentages of carbon black, while the virgin additive is a pure SBR compound without any fillers. This heterogeneity in composition makes the recycled additive perform better as a reinforcing agent, since carbon black can migrate to the rubber matrix [11,42]. Besides these compositional differences, it is shown that the broken free chains on the surface of the recycled additive play a decisive role in the mechanical performance of the samples, especially in the pristine state. As mentioned above this effect can be attributed to the improved compatibility and to the effective transmission of stress between the matrix and the filler. As for the healed state, although it is expected that additional GTR loadings (i.e., carbon black and fully cross-linked particles) may be an impediment to the self-healing process, the tensile strength is maintained and increases slightly at higher Factor C values (see Fig. 5 (a)). Thus, it can be confirmed that the effect of the decreasing network density counteracts the negative effect of the loading in the healed state.

3.4. Optimisation test

Fig. 5 (b) represents the tensile strength for the pristine (solid line) and healed state (dashed line) of SBR formulations reinforced

Table 5
Mechanical properties of the formulations studied for validation and optimisation.

Run	Additive	Factor A	Factor B (phr)	Factor C (%)	Factor D (%)	Pristine state			Healed state			̑ (%) ^a						
						M _{50%} (MPa)	M _{100%} (MPa)	̑ _b (%)	̑ _{max} (MPa)	M _{50%} (MPa)	M _{100%} (MPa)	̑ _b (%)	̑ _{max} (MPa)	M _{50%}	M _{100%}	̑ _b	̑ _{max}	
Validation	Virgin	13	S0.7	WJ	20	87	100 ^b	0.46 ± 0.01	0.59 ± 0.01	448.6 ± 17.5	1.58 ± 0.09	0.50 ± 0.01	0.71 ± 0.02	102.9 ± 9.5	0.64 ± 0.06	23	48	
	14	S1	WJ	20	57	100 ^b	0.44 ± 0.01	0.54 ± 0.01	474.0 ± 23.4	1.45 ± 0.11	0.47 ± 0.01	-	73.9 ± 7.7	0.60 ± 0.02	106	16	38	
	15	S2	WJ	20	0	100 ^b	0.42 ± 0.01	0.51 ± 0.01	426.5 ± 21.7	1.19 ± 0.05	0.46 ± 0.02	-	73.6 ± 7.3	0.52 ± 0.03	109	17	44	
	Recycled	16	GTR_WJ	WJ	20	0	100	0.49 ± 0.01	0.57 ± 0.01	671.0 ± 26.8	1.86 ± 0.07	0.52 ± 0.02	-	62.2 ± 4.0	0.66 ± 0.05	106	8	30
	17	dWJ_71°C	WJ	20	22	100	0.53 ± 0.02	0.61 ± 0.02	763.7 ± 45.3	2.18 ± 0.04	0.57 ± 0.02	0.68 ± 0.03	148.8 ± 14.0	0.75 ± 0.01	107	111	19	34
	18	dWJ_200°C	WJ	20	63	0	0.46 ± 0.02	0.56 ± 0.03	673.8 ± 41.3	2.71 ± 0.19	0.55 ± 0.01	-	70.0 ± 6.3	0.92 ± 0.03	119	10	10	
	Optimisation	19	dWJ_200°C	WJ	10	63	0	0.45 ± 0.03	0.57 ± 0.04	503.3 ± 22.3	1.83 ± 0.14	0.57 ± 0.03	-	68.8 ± 6.1	0.80 ± 0.03	126	14	33
	18	dWJ_200°C	WJ	20	63	0	0.46 ± 0.02	0.56 ± 0.03	673.8 ± 41.3	2.71 ± 0.19	0.55 ± 0.01	-	70.0 ± 6.3	0.92 ± 0.03	119	10	23	
	20	dWJ_200°C	WJ	30	63	0	0.47 ± 0.01	0.59 ± 0.01	797.3 ± 25.7	3.82 ± 0.15	0.57 ± 0.02	0.74 ± 0.02	100.2 ± 5.0	0.95 ± 0.05	121	125	13	19
	21	dWJ_200°C	WJ	40	63	0	0.46 ± 0.01	0.58 ± 0.02	875.1 ± 52.4	3.91 ± 0.29	0.56 ± 0.02	0.71 ± 0.05	98.7 ± 5.3	1.20 ± 0.02	121	122	11	18

^a Standard deviation (St Dev) < 0.1.

^b These samples correspond to the virgin additive, 100% selectivity is assumed for the non-crosslinked free chains.

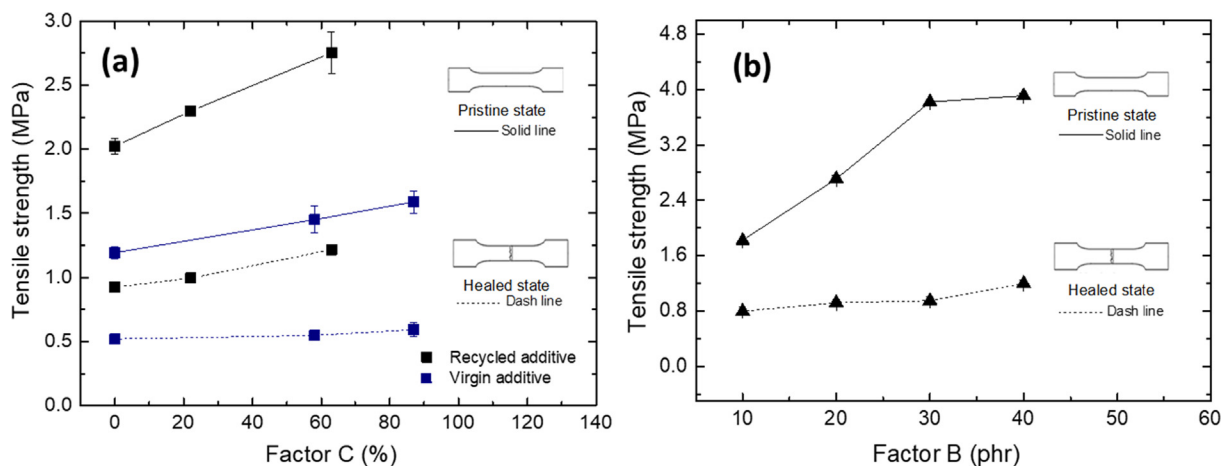


Fig. 5. Tensile strength for (a) samples reinforced with virgin vs. recycled additives and (b) optimised formulations.

with a recycled additive, whose Factor C (decrease in network density) has been increased to 63%. The tensile strength was plotted as a function of Factor B (loading) to demonstrate the factorial design optimisation recommendations. In all cases, the particles with the highest surface area (WJ) were used to work under the most optimal conditions, as indicated by the model. All the tensile strength values plotted in Fig. 5 (b) exceed the mean values shown in the main effect curves in Fig. 3 (a) (1.1 MPa for the pristine state and 0.6 MPa for the healed state). They even reach values of 3.9 MPa (almost 4 times) and 1.2 MPa (twice) for the pristine and healed state, respectively (see Table 4). This is an important optimisation evidence based mainly on increasing Factor C, as predicted by the contour plots in Fig. 4. In addition, increasing Factor C enabled increasing Factor B, further maximising tensile strength.

Fig. 5 (b) also shows small increases in tensile strength in the healed state with increasing loading. Once again, it can be shown that the negative effect of loading on the healed state is attenuated by increasing Factor C. However, the rate of improvement of the healed state is lower than that of the pristine state when Factor B is increased. Consequently, the difference in tensile strength between both states is higher, reducing the healing efficiency.

Fig. 6 shows optical micrographs of the SBR formulations, with the aim of relating the factors studied with the morphologies obtained. It can be seen how by increasing Factor A (surface area, see orange line) a more homogeneous morphology is achieved. At equal surface area (WJ) particles, if the decrease of the lattice density is increased from 0 to 22% (see green line), the homogeneity of the mixture is even higher. The reinforcing phase can hardly

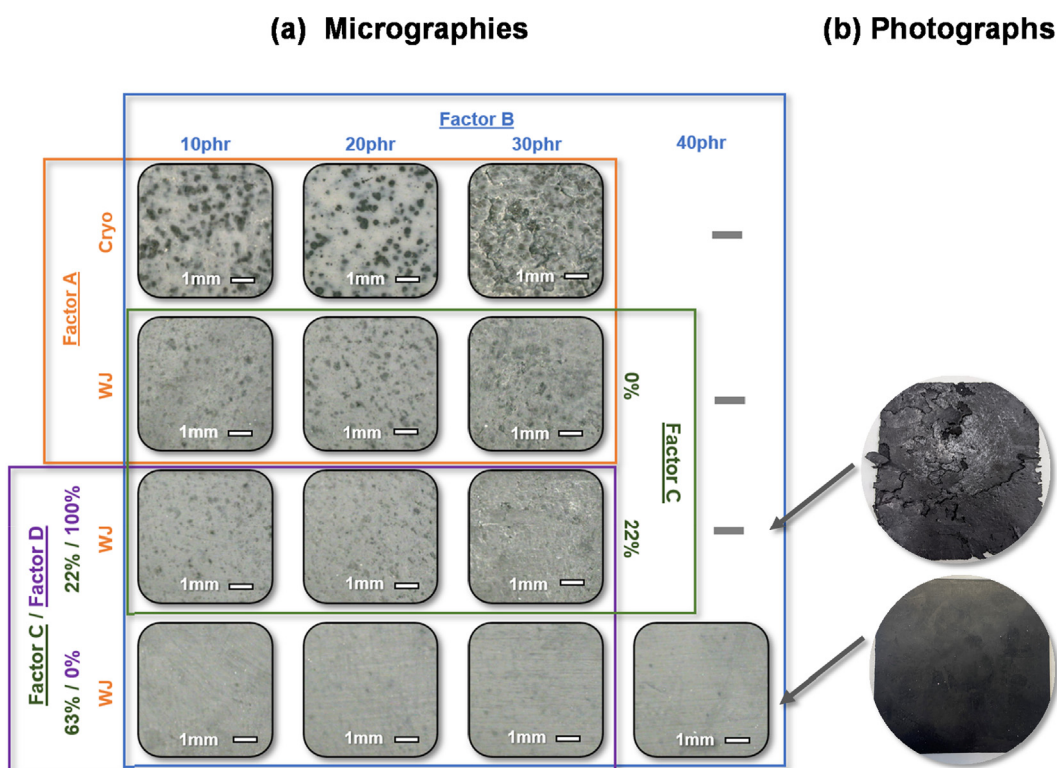


Fig. 6. (a) Micrographs of the samples obtained by changing the different DoE factors (b) Photographs of selected specimens.

be visible. In none of the above cases, it was possible to obtain formulations with additive content higher than 30%. As can be seen in the photographs in Fig. 6 b, there is poor compaction of the compound when the Factor C is less than 22%. However, by increasing Factor C from 22% to 63%, regardless of the selectivity of the network breakage (see purple line), not only does the homogeneity of the samples improve significantly, but also compounds with

40% GTR can be produced with a good surface finish and compaction.

Finally, although it was not possible to predict with the factorial analysis the behaviour of mechanical properties such as elongation at break and Modulus as a function of the factors studied, the corresponding responses for these properties and their repair efficiency were plotted in Fig. 7. An attempt has been made to

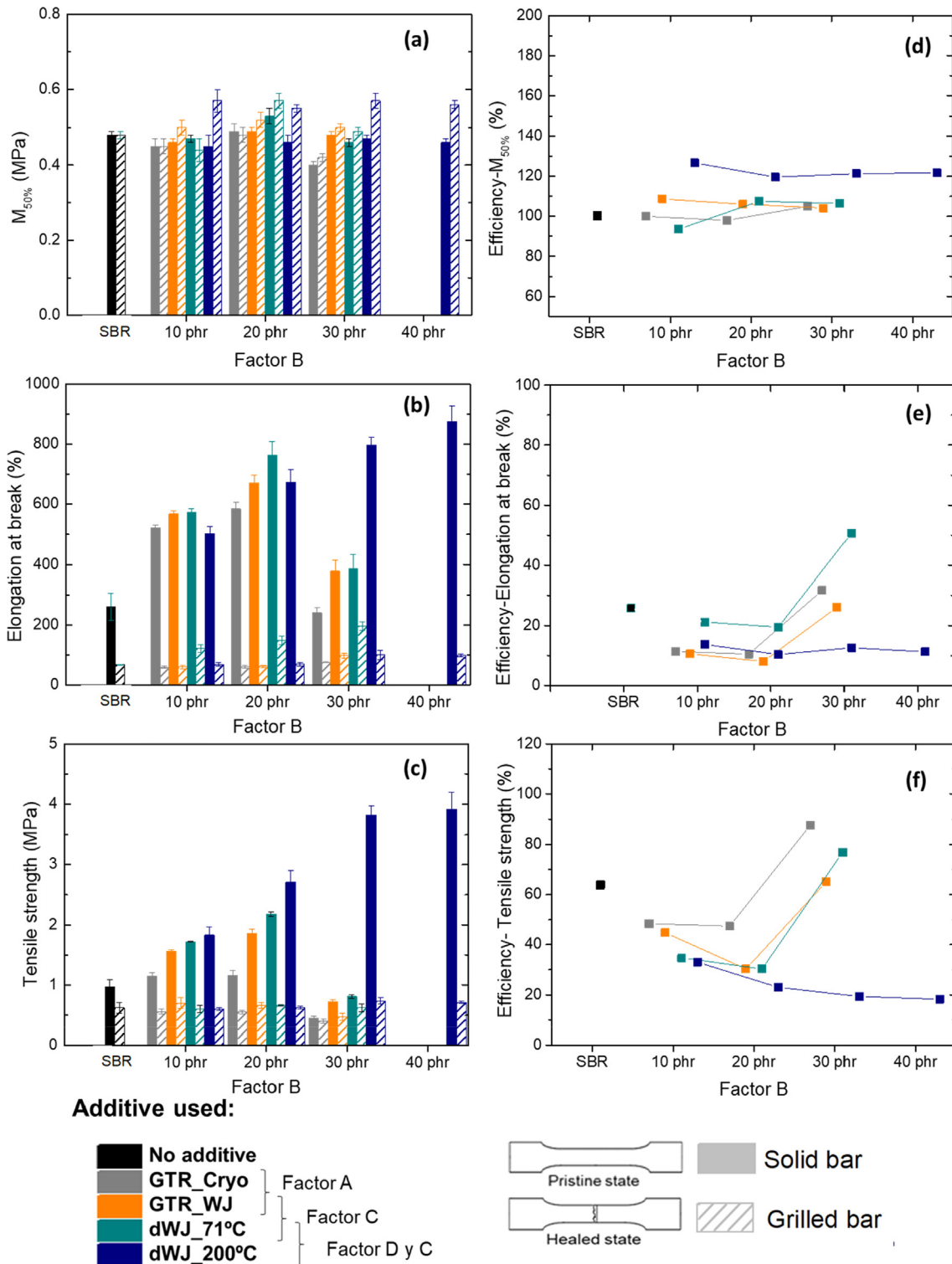


Fig. 7. Influence of Factors A, B, C and D on (a) Modulus at 50% elongation, (b) Elongation at break (c) Tensile strength; Repair efficiency based on (d) Modulus at 50% elongation, (e) Elongation at break, (f) Tensile strength.

predict graphically the effect of each factor and to see the overall mechanical behaviour of the materials obtained. Furthermore, these properties are compared with an unfilled SBR compound (bars and black dots in Fig. 7).

In the case of modulus, as already described, there are practically no variations because it has been measured at very low deformations (see Fig. 7 (a)). This, together with the low values and errors that an elastomer presents per se, due to its cross-linked network in comparison with other polymers, makes it impossible to establish comparisons within the range studied. Additionally, the efficiencies that were measured from Modulus at 50% are values that exceed 100% (Fig. 7 (d)). These values are physically meaningless. Authors such as Araujo-Morera J. et al [37] proposed a thermal treatment to the pristine state to correct this measurement, in our case it was not relevant.

With regard to elongation at break and tensile strength, it seems beneficial to use GTR with high surface areas either in pristine or healed state (the values are always higher for the orange bars if compared to the grey bars, see Fig. 7 (b) and (c)). The same occurs when there is an increase in Factor C, as already discussed (compare orange and green bars in Fig. 7 (b) and (c)). However, regardless of particle morphology, for 30 phr of additive, the compounds show a drop in both tensile strength and elongation at break, especially for the pristine state. This loss of properties reduces the gap between the pristine and healed state, so the healing efficiencies are generally higher for the compounds with 30 phr of additive (see Fig. 7 (e) and (f)). The results show that only by optimizing Factor C (blue bar, Fig. 7 (b) and (c)) can high property values be achieved again, as predicted by the factorial for the tensile strength. Fig. 7 (b) shows evidence that this also applies to the elongation at break.

Finally, although increasing the Factor C is determinant for improving mechanical properties in the pristine and healed state, the rate of improvement of the pristine state is higher and must be considered when determining an optimal healing efficiency.

4. Conclusions

The mechanical properties of self-healing SBR compounds reinforced with GTR were assessed. The influence of the microstructural characteristics of GTR on the mechanical performance was studied through a statistical analysis based on a DoE methodology. Due to the complexity of the study, two full factorials were designed. It was possible to establish that Factor C (decreasing network density) and its interactions with Factor A (surface area) and Factor B (filler amount) were statistically significant for the tensile strength. This is due to the improved compatibility that comes up with a larger volume of free chains on the surface of the reinforcing additive for interacting with the SBR matrix. The p-values obtained were, in all cases, less than 0.05; while the determination coefficient (R^2) exceeded 98% in all the conditions studied. This demonstrates the reliability of the factorial response. Moreover, the major influence of Factor C on tensile strength was validated when a virgin additive with low crosslinking degree was tested.

The main effect study showed that the antagonism between the tensile strength in the pristine state and the healed state is given by the amount of additive (Factor B). Significant amounts of GTR maximize the stiffness in the pristine state but are physical defects for the self-healing process. This effect can be attenuated, in the healed state, by considerably increasing Factor C; however, the increase of Factor C produces, at the same time, a dramatic improvement in the pristine state which results in a notorious loss of healing efficiency.

A priori, it has not been possible to demonstrate that the free long chains on the GTR surface resulting from selective devulcani-

sation (Factor D) can play a major role in the overall mechanical performance of self-healing composites.

Funding

This research was funded by UVA Postdoctoral Contract CONVOCATORIA 2020 (K.C.N.C) and by the State Research Agency of Spain (AEI) through grants RYC2017-22837 (M.H.S.) and PRE2018-084732 (L.E.A.P.).

CRedit authorship contribution statement

Karina C. Nuñez Carrero: Conceptualization, Validation, Writing – review & editing, Visualization, Formal analysis, Project administration, Funding acquisition. **Luis E. Alonso Pastor:** Methodology, Validation, Investigation, Data curation. **Marianella Hernández Santana:** Conceptualization, Validation, Resources, Data curation, Writing – review & editing, Visualization, Supervision, Project administration, Funding acquisition. **José María Pastor:** Supervision, Project administration, Funding acquisition.

Declaration of Competing Interest

The authors declare that they have no known competing financial interests or personal relationships that could have appeared to influence the work reported in this paper.

Acknowledgments

All the authors acknowledge Lehigh Technologies and Rubber Jet for kindly providing GTR samples.

Appendix A. Supplementary material

Supplementary data to this article can be found online at <https://doi.org/10.1016/j.matdes.2022.110909>.

References

- [1] S.R. White, N.R. Sottos, P.H. Geubelle, J.S. Moore, M.R. Kessler, S.R. Sriram, E.N. Brown, S. Viswanathan, Autonomic Healing of Polymer Composites, *Nature*. 409 (2001) 794. <https://www.nature.com/articles/35057232.pdf>.
- [2] V. Restrepo, R.V. Martinez, Bioinspired fabrication of reconfigurable elastomeric cementitious structures using self-healing mechanical adhesives interfaces, *Mater. Des.* 205 (2021), <https://doi.org/10.1016/j.matdes.2021.109691> 109691.
- [3] X. Yang, L. Guo, X. Xu, S. Shang, H. Liu, A fully bio-based epoxy vitrimer: Self-healing, triple-shape memory and reprocessing triggered by dynamic covalent bond exchange, *Mater. Des.* 186 (2020) 1–10, <https://doi.org/10.1016/j.matdes.2019.108248>.
- [4] P. Cordier, F. Tournilhac, C. Soulié-Ziakovic, L. Leibler, Self-healing and thermoreversible rubber from supramolecular assembly, *Nature*. 451 (2008) 977–980, <https://doi.org/10.1038/nature06669>.
- [5] M. Hernández, M. Mar Bernal, A.M. Grande, N. Zhong, S. Van Der Zwaag, S.J. García, Effect of graphene content on the restoration of mechanical, electrical and thermal functionalities of a self-healing natural rubber, *Smart Mater. Struct.* 26 (2017), <https://doi.org/10.1088/1361-665X/aa71f5>.
- [6] G. Lai, Y. Li, G. Li, Effect of concentration and temperature on the rheological behavior of collagen solution, *Int. J. Biol. Macromol.* 42 (2008) 285–291, <https://doi.org/10.1016/j.ijbiomac.2007.12.010>.
- [7] T. Wan, D. Chen, Mechanical enhancement of self-healing waterborne polyurethane by graphene oxide, *Prog. Org. Coatings*. 121 (2018) 73–79, <https://doi.org/10.1016/j.porgcoat.2018.04.016>.
- [8] Y. Xu, D. Chen, Self-healing polyurethane/attapulgite nanocomposites based on disulfide bonds and shape memory effect, *Mater. Chem. Phys.* 195 (2017) 40–48, <https://doi.org/10.1016/j.matchemphys.2017.04.007>.
- [9] X. Kuang, G. Liu, X. Dong, D. Wang, Enhancement of Mechanical and Self-Healing Performance in Multiwall Carbon Nanotube/Rubber Composites via Diels-Alder Bonding, *Macromol. Mater. Eng.* 301 (2016) 535–541, <https://doi.org/10.1002/mame.201500425>.
- [10] M. Hernández Santana, M. Huet, P. Lameda, J. Araujo, R. Verdejo, M.A. López-Manchado, Design of a new generation of sustainable SBR compounds with good trade-off between mechanical properties and self-healing ability, *Eur.*

- Polym. J. 106 (2018) 273–283, <https://doi.org/10.1016/j.eurpolymj.2018.07.040>.
- [11] L.E. Alonso Pastor, K.C. Nuñez Carrero, J. Araujo-Morera, M. Hernández Santana, J.M. Pastor, Setting relationships between structure and devulcanization of ground tire rubber and their effect on self-healing elastomers, *Polymers (Basel)* 14 (2022), <https://doi.org/10.3390/polym14010011>.
- [12] R. Saputra, R. Walvekar, M. Khalid, N. Mujawar, C. Science, N. Jalan, S. Jaya, Chemosphere Current progress in waste tire rubber devulcanization Mika Sillanpää, 265 (2021), 10.1016/j.chemosphere.2020.129033.
- [13] K. Formela, A. Hejna, L. Zedler, X. Colom, J. Cañavate, Microwave treatment in waste rubber recycling – recent advances and limitations, 13 (2019) 565–588.
- [14] D. Verdine, G.A. Oliver, F.A. de Almeida, M. de Lourdes Noronha, G.F. Gomes, Analysis of the properties of the self-compacting concrete mixed with tire rubber waste based on design of experiments, *Structures*. 33 (2021) 3461–3474, <https://doi.org/10.1016/j.istruc.2021.06.076>.
- [15] D. Montgomery, *Design and Analysis of Experiments*, fifth edit, 2001.
- [16] I. Mangili, M. Oliveri, M. Anzano, E. Collina, D. Pitea, M. Lasagni, Full factorial experimental design to study the devulcanization of ground tire rubber in supercritical carbon dioxide, *J. Supercrit. Fluids*. 92 (2014) 249–256, <https://doi.org/10.1016/j.supflu.2014.06.001>.
- [17] B.M. Meysami M, C. Tzoganakis, P. Mutyala, S.H. Zhu, Devulcanization of Scrap Tire Rubber with Supercritical CO₂: A Study of the Effects of Process Parameters on the Properties of Devulcanized Rubber, *Int. Polym. Process*. 32 (2017) 183–93.
- [18] Z.X. Xin, Z.X. Zhang, K. Pal, J.U. Byeon, S.H. Lee, J.K. Kim, Study of microcellular injection-molded polypropylene/waste ground rubber tire powder blend, *Mater. Des.* 31 (2010) 589–593, <https://doi.org/10.1016/j.matdes.2009.07.002>.
- [19] M. Salehi, J.W.M. Noordermeer, L.A.E.M. Reuvekamp, A. Blume, Parameter optimization for a laboratory friction tester to predict tire ABS braking distance using design of experiments, *Mater. Des.* 194 (2020), <https://doi.org/10.1016/j.matdes.2020.108879> 108879.
- [20] O.K. Klaus Hinkelmann, *Design and Analysis of Experiments: Introduction to Experimental Design*, Second Edi, 2008. 10.1002/9780470191750.
- [21] P.J. Flory, *Principles of polymer chemistry*, Cornell Univ. Press, Ithaca, NY, 1953.
- [22] P.J. Flory, J. Rehner, Statistical mechanics of cross-linked polymer networks I. Rubberlike elasticity, *J. Chem. Phys.* 11 (11) (1943) 512–520.
- [23] M.M. Horikx, Chain Scissions in a Polymer Network, *XIX 19 (93) (1956) 445–454*.
- [24] D.W. Edwards, B. Danon, P. van der Gryp, J.F. Görgens, Quantifying and comparing the selectivity for crosslink scission in mechanical and mechanochemical devulcanization processes, *J. Appl. Polym. Sci.* 133 (2016) 1–10, <https://doi.org/10.1002/app.43932>.
- [25] S. Seghar, L. Asaro, N. Ait Hocine, Experimental Validation of the Horikx Theory to be Used in the Rubber Devulcanization Analysis, *J. Polym. Environ.* 27 (2019) 2318–2323, <https://doi.org/10.1007/s10924-019-01513-z>.
- [26] M. Hernández Santana, M. den Brabander, S. García, S., van der Zwaag, Routes to Make Natural Rubber Heal: A Review, *Polym. Rev.* 58 (2018) 585–609, <https://doi.org/10.1080/15583724.2018.1454947>.
- [27] Minitab Inc., Interpret the key results for Main Effects Plot., (2022) <https://support.minitab.com/en-us/minitab-express/>.
- [28] T.D. Sreeja, S.K.N. Kutty, Cure characteristics and mechanical properties of natural rubber/reclaimed rubber blends, *Polym. - Plast. Technol. Eng.* 39 (2000) 501–512, <https://doi.org/10.1081/PPT-100100043>.
- [29] T.D. Sreeja, S.K.N. Kutty, Styrene butadiene rubber / reclaimed rubber blends, 4037 (2010). 10.1080/00914030304902.
- [30] S. Ramarad, M. Khalid, C.T. Ratnam, A.L. Chuah, W. Rashmi, Waste tire rubber in polymer blends: A review on the evolution, properties and future, *Prog. Mater. Sci.* 72 (2015) 100–140, <https://doi.org/10.1016/j.pmatsci.2015.02.004>.
- [31] M.D.H. Stefan Bode, Marcel Enke, Marianella Hernandez, Ranjita K. Bose, Antonio M. Grande, Sybrand van der Zwaag, Ulrich S. Schubert, Santiago J. Garcia, Characterization of self-healing polymers: From macroscopic healing tests to the molecular mechanism, *Adv. Polym. Sci.* 273 (2016) 113–142.
- [32] K. Balasundaram, M. Sharma, Investigations into a thiol-impregnated CaCO₃-based adsorbent for mercury removal: a full factorial design approach, *RSC Adv.* 5 (2015) 73868–73874, <https://doi.org/10.1039/c5ra10902g>.
- [33] M.H. Wu, C. F. J., *Experiments: Planning, Analysis, and Parameter Design Optimization*, 2000.
- [34] J. Frost, Multiple regression analysis: use adjusted R-squared and predicted R-squared to include the correct number of variables Minitab Blog, (2013) <https://blog.minitab.com/blog/adventures-in-statistics>.
- [35] S. Ramarad, M. Khalid, C.T. Ratnam, A.L. Chuah, W. Rashmi, Progress in Materials Science Waste tire rubber in polymer blends : A review on the evolution, properties and future, *J. Prog. Mater. Sci.* 72 (2015) 100–140, <https://doi.org/10.1016/j.pmatsci.2015.02.004>.
- [36] A. Yehia, E.M. Abdelbary, M. Mull, M.N. Ismail, Y. Hefny, New Trends for Utilization of Rubber Wastes, (2012) 5–14. 10.1002/masy.201251001.
- [37] R. Verdejo, M. Hern, J. Araujo-morera, A.L. Miguel, Unravelling the effect of healing conditions and vulcanizing additives on the healing performance of rubber networks, 238 (2022). 10.1016/j.polymer.2021.124399.
- [38] M.H. Santana, M. Huete, P. Lameda, J. Araujo, R. Verdejo, M.A. López-manchado, Design of a new generation of sustainable SBR compounds with good trade-off between mechanical properties and self-healing ability, *Eur. Polym. J.* 106 (2018) 273–283, <https://doi.org/10.1016/j.eurpolymj.2018.07.040>.
- [39] J. Shi, K. Jiang, D. Ren, H. Zou, Y. Wang, X. Lv, L. Zhang, Structure and Performance of Reclaimed Rubber Obtained by Different Methods (2013) 999–1007, <https://doi.org/10.1002/app.38727>.
- [40] B. Adhikari, S. Maiti, Reclamation and recycling of waste rubber, 25 (2000) 909–948.
- [41] V. Nagarajan, A.K. Mohanty, M. Misra, Reactive compatibilization of poly trimethylene terephthalate (PTT) and polylactic acid (PLA) using terpolymer : Factorial design optimization of mechanical properties, *Mater. Des.* 110 (2016) 581–591, <https://doi.org/10.1016/j.matdes.2016.08.022>.
- [42] P. Song, C. Wan, Y. Xie, K. Formela, S. Wang, Vegetable derived-oil facilitating carbon black migration from waste tire rubbers and its reinforcement effect, *Waste Manag.* 78 (2018) 238–248, <https://doi.org/10.1016/j.wasman.2018.05.054>.